Journal of Biomechanics 46 (2013) 1081–1087

Contents lists available at SciVerse ScienceDirect

Journal of Biomechanics

journal homepage: www.elsevier.com/locate/jbiomech
www.JBiomech.com

The effects of confluency on cell mechanical properties

Yu.M. Efremov*, A.A. Dokrunova, D.V. Bagrov, K.S. Kudryashova, O.S. Sokolova, K.V. Shaitan

M.V. Lomonosov Moscow State University, Faculty of Biology, Department of Bioengineering, Leninskie Gory, 1/73, 111991 Moscow, Russia

ARTICLE INFO

Article history:
Accepted 21 January 2013

Keywords:
AFM
Vero cells
Viscoelasticity
Confluency
Actin cytoskeleton

ABSTRACT

Mechanical properties of cells depend on various external and internal factors, like substrate stiffness and surface modifications, cell ageing and disease state. Some other currently unknown factors may exist. In this study we used force spectroscopy by AFM, confocal microscopy and flow cytometry to investigate the difference between single non-confluent and confluent (in monolayer) Vero cells. In all cases the stiffness values were fitted by log-normal rather than normal distribution. Log-normal distribution was also found for an amount of cortical actin in cells by flow cytometry. Cells in the monolayer were characterized by a significantly lower (1.4–1.7 times) Young's modulus and amount of cortical actin than in either of the single non-confluent cells or cells migrating in the experimental wound. Young's modulus as a function of indentation speed followed a weak power law for all the studied cell states, while the value of the exponent was higher for cells growing in monolayer. These results show that intercellular contacts and cell motile state significantly influence the cell mechanical properties.

1. Introduction

Atomic force microscopy (AFM) is widely used in biological studies for visualization of biomolecules (Engel and Muller, 2000; Graham et al., 2010) and cells (Costa, 2006; Efremov et al., 2011; Rotsch and Radmacher, 2000) and for the assessment of their mechanical characteristics (Kuznetsova et al., 2007; Rico et al., 2008; Takai et al., 2005). Force spectroscopy of cells by AFM, along with other techniques like the optical stretcher (Guck et al., 2005), micropipette aspiration (Ward et al., 1991), magnetic twisting cytometry (Alenghat et al., 2000) and laser tracking microrheology (Hoffman et al., 2006), is an important source of information about cell mechanical properties. The data about cell mechanical properties combined with confocal microscopy data confirm that the cytoskeleton, mainly the actin network, contributes significantly to cell stiffness (Guck et al., 2005; Mackay et al., 2012; Rotsch and Radmacher, 2000). It has been shown, that changes in cell stiffness are closely related to cell type and various external and internal conditions, like substrate stiffness (Franze et al., 2009; Mackay et al., 2012; Solon et al., 2007) and surface modifications (Takai et al., 2005), cell ageing (Starodubtseva, 2011) and disease state (Lekka et al., 2012). However, the elasticity modulus values measured by AFM additionally depend on several factors, including force loading rate, indentation depth, probe geometry, models for force curve approximation, properties of the substrates used for cell growth and others (Lekka et al., 2012; Mahaffy et al., 2000; Rico et al., 2008). Their influence on the elastic properties of cells must be considered for a proper evaluation and for further comparison of data obtained in different experiments.

In vivo cells stay in close connection with each other in the tissues and continuously exchange signals with neighboring cells (Lodish et al., 2000). Cells, cultivated on a flat substrate *in vitro*, are deprived of some of those signals. Single non-confluent cells are deprived more than cells in a monolayer, where signaling information can be shared by neighboring cells with intercellular contacts. These molecular or mechanical signals may lead to different properties of non-motile cells in monolayer (Yeung et al., 2005) and single non-confluent cells. On the other hand, transition from a non-motile to a motile state is accompanied by polarization of cells. Various signaling and structural proteins operating together lead to the reorganization of the actin cytoskeleton (Kole et al., 2005; Ridley et al., 2003).

We used the African green monkey *Cercopitecus aethiops* kidney cell line (Vero) as a model system to determine the effects of confluency on the mechanical properties of cells. Vero cells are widely used in various areas of biology and biotechnology. They are used as substrates for viral vaccine manufacture (Barrett et al., 2009; Ehrlich et al., 2012), for virus detection (Macfarlane and Sommerville, 1969), for detection of verotoxin (Maniar et al., 1990), as substrates

* Correspondence to: M.V. Lomonosov Moscow State University, Faculty of Biology, Department of Bioengineering, Leninskie Gory, 1/73, 111991 Moscow, Russia. Tel./fax: +79459395738.
E-mail addresses: yu.efremov@gmail.com, efremov@mail.bio.msu.ru (Yu.M. Efremov), aitsanochka-79@yandex.ru (A.A. Dokrunova), dbagrov@gmail.com (D.V. Bagrov), rekamoskva@mail.ru (K.S. Kudryashova), sokolova184@gmail.com (O.S. Sokolova), shaitan@moldyn.org (K.V. Shaitan).

0021-9290/$ - see front matter © 2013 Elsevier Ltd. All rights reserved.
http://dx.doi.org/10.1016/j.jbiomech.2013.01.022

for human early round spermatids differentiation (Tanaka et al., 2009) and for the improvement of mouse (Lai et al., 1992) and human early embryo development (Menezo et al., 1990). Vero are non-polarized epithelial cells, which have a typical fibroblastoid shape and form a well-defined flat monolayer. The mechanism by which Vero cells became immortal is still unknown. During tissue-culture passage (at the high passage levels, $p > 200$), Vero cells can develop the capacity to form tumors (Manohar et al., 2008).

Here, we determined the mechanical properties of single non-confluent Vero cells by AFM and compared it with the properties of fully confluent cells (in monolayer). The single cells were prepared either by seeding or by wound healing assay, when cells migrated into the scratch wound from monolayer (Valster et al., 2005). Confocal microscopy and flow cytometry were used to assess the changes in the actin cytoskeleton organization and actin amount.

2. Materials and methods

2.1. Cell culture and confocal microscopy

Vero cells were grown in DMEM medium (PanEco, Russia) supplemented with 10% fetal bovine serum (FBS) (HyClone, USA) at 37 °C in a humidified 5% CO_2 atmosphere in an incubator (Sanyo, Japan). For AFM imaging and force spectroscopy, the cells were harvested from the subculture, seeded on sterile 35 mm Petri dishes and placed into the incubator. For the experiments with single non-confluent cells they were grown for 1–2 days, for the experiments with a monolayer—for 3–4 days. The monolayer wounding was used to examine cell elasticity during migration inside the wound (Valster et al., 2005). Two (or more) parallel scratch wounds of approximately 400 μm width were made with a blue pipette tip (Greiner Bio-one, Germany), the growth medium was replaced and cells were incubated for several hours before AFM measurements.

For the confocal fluorescence imaging, cells were seeded on sterile 35 mm glass bottom Petri dishes (Greiner Bio-one, Germany). The filamentous actin (F-actin) was labeled with rhodamine phalloidin (Molecular Probes, Europe). Fluorescence images were taken using a Zeiss LSM510 Meta inverted confocal microscope (Carl Zeiss, Germany).

2.2. Flow cytometry

Flow cytometric measurements for single non-confluent cells and cells in monolayer were performed on a Cytomics FC500 flow cytometer (Beckman Coulter, USA). Cells were harvested by trypsinization, diluted to 1,000,000 cells/ml in PBS (Amresco, USA), fixed with 4% paraformaldehyde (Fluka, Germany), permeabilized with 0.1% Triton X-100 (Loba Chemie, Austria) in PBS and stained with rhodamine phalloidin (one set of experiments) or Alexa Fluor 488 phalloidin (Molecular Probes, Europe; two sets of experiments). Actin staining was checked by confocal microscopy. Cells without staining were used as negative control. Integral (total signal per cell) forward and sideward scatter intensities and integral green fluorescence intensity for Alexa Fluor 488 phalloidin staining (FL-1 channel) or integral red fluorescence intensity for rhodamine phalloidin staining (FL-3 channel) of the samples were measured. Near 20,000 cells/sample were analyzed.

2.3. Atomic force microscopy and force spectroscopy

The AFM measurements were performed at room temperature using a commercial atomic force microscope Solver Bio (NT-MDT, Russia) combined with an inverted optical microscope (Olympus, Japan). Just before the AFM measurements the growth medium was replaced by PBS. We used silicon nitride triangular cantilevers MSCT-AUHW (former Veeco Instruments, now Bruker, USA) in contact mode for imaging of living cells. The typical curvature radius of the tips is 10 nm, the length, width, and thickness of the cantilevers are 310, 15, and 0.55 μm, respectively, and force constant $k = 0.01$ N/m.

For the force spectroscopy experiments we used the tipless AFM probes CSG11 (NT-MDT, Russia) glued with a 9 μm diameter polystyrene bead. To measure Young's modulus (elastic modulus, stiffness, E) 3–5 force were taken at 1 μm/s rate on each of the studied cells near its center, where the cell height is large enough to apply the Hertz model for data processing. The elastic moduli obtained from these curves were averaged to give the E value for each cell. For each of the non-confluent cell states (formed by seeding or by wound healing assay) three independent experiments were conducted, 15–25 cells were analyzed in each experiment. During experiments with the cell monolayer 15–20 force curves were taken on each of 4–5 areas (400–500 μm diameter), because of the rather small cell projection area. Hertz's contact model was applied for data processing (see Supplementary information for details). To compare the mechanical properties of cells in different states, E was measured at fixed indentation speed (1 μm/s) and at fixed indentation depth (500 nm).

2.4. Analysis of cell viscoelastic properties

To characterize the viscoelastic behavior of cells we measured their mechanical response at varying indentation rates (0.25–8 μm/s), as described in the work by Nawaz et al. (2012). Due to significant difference between the cantilever spring constant and the cellular spring constant we admitted that the cell indentation speed is identical to the piezo movement speed.

Besides, we measured the loss tangents (or hysteresivity) of cells. Sinusoidal perturbation with small amplitude (less than 20 nm) and low frequency (0.3 Hz) was added to the vertical scan control voltage after indentation to 500 nm depth. The cantilever deflection (stress) and scanner Z position (strain) were sampled at ~200 Hz for 50 s. The Fast Fourier transform analyses were used to determine phase shift between stress and strain (Alcaraz et al., 2003; Rico et al., 2005). When calculated this way, η does not depend on k, v and R and other uncertainties associated with Hertzian contact mechanics (Alcaraz et al., 2003). The calculated loss tangent (tangent of the phase shift) provides a measure of solidlike ($\eta < 1$) or fluidlike ($\eta > 1$) behavior of the cell. Given the low oscillatory frequency applied (0.3 Hz), we neglected the hydrodynamic drag influence (Alcaraz et al., 2002). At least 10 cells in each state were analyzed to obtain the indentation rate dependences of E and η. Data were processed with Origin software (OriginLab Corp., Northampton, MA, USA). All AFM experiments were performed during a 30–40 min period. Cell detachment and viability decrease started only after 3–4 h as determined by the trypan blue exclusion test (Strober, 2001).

2.5. Statistical analysis

The non-parametric Mann–Whitney U test was used to determine if differences existed between the groups. The Shapiro–Wilk test was used for the normality test. Analysis was performed using Statistica software, version 8.0 (StatSoft, USA). Young's modulus values were log-normally distributed (meaning that the logarithms were normally distributed) and thus were described using geometric means and multiplicative standard deviations (see below).

3. Results

3.1. Morphology and cytoskeleton structure of Vero cells in different states

The single cells were prepared either by seeding or by wound healing assay, when cells migrated into the scratch wound from

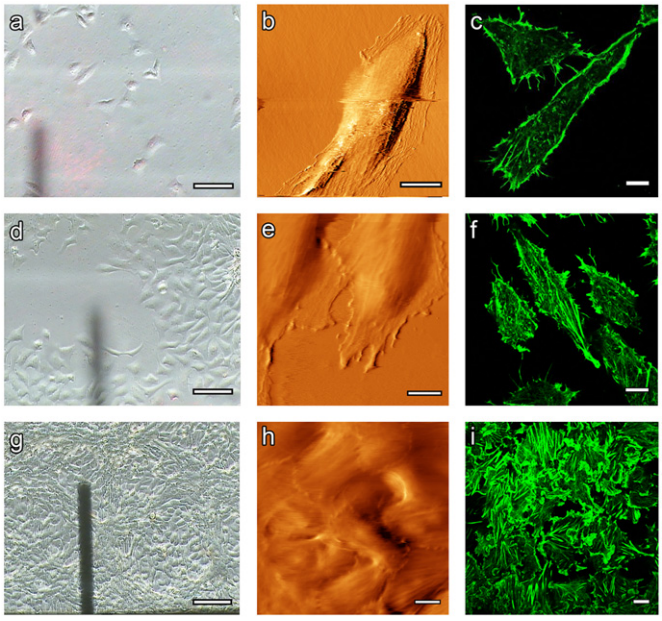

Fig. 1. Bright field images (a, d, and g), AFM deflection images (b, e, and h) and confocal images (c, f, and i) of Vero cells. (a–c) Single cells, (d–f) cells in wound, and (g–i) cells in monolayer. The shadow of the cantilever is seen on the bright field images. Scale bar represents 100 μm on bright field images and 10 μm on the others.

monolayer (Valster et al., 2005). The bright field and AFM images of non-confluent single cells, cells in a monolayer and cells in the experimental wound are compared in Fig. 1. The overall cytoskeleton structure was quite similar in all studied cell states: the majority of stress fibers were located at the basal part of the cell just above the substrate (Fig. 1c, f, and i). Cells being cultivated in the monolayer

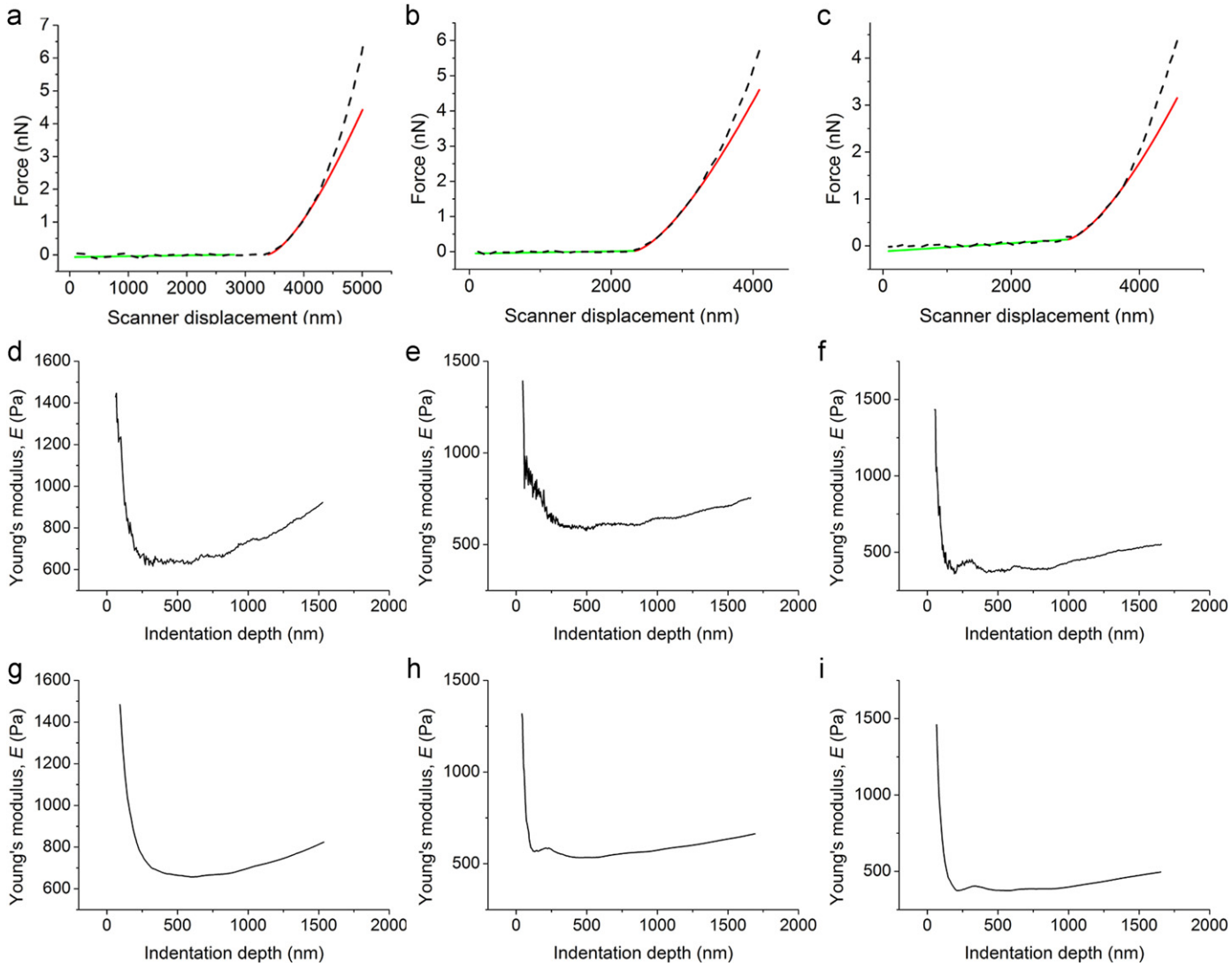

Fig. 2. (a), (d), and (c)—Typical force curves at 1 μm/s speed obtained on single non-confluent (a), migrating in wound (b) and cells in monolayer (c). The first 500 nm of indentation were fitted with the Hertz model's equation (red line—after the contact point, green line—the non-contact region). (d), (e), and (f) —Indentation dependences of *E*, estimated from the Hertz model's equation for these force curves. (g), (h), and (i)—Indentation dependences of *E* for the same experiments, estimated from force curves fitting as a function of indentation depth. (For interpretation of the references to color in this figure legend, the reader is referred to the web version of this article.)

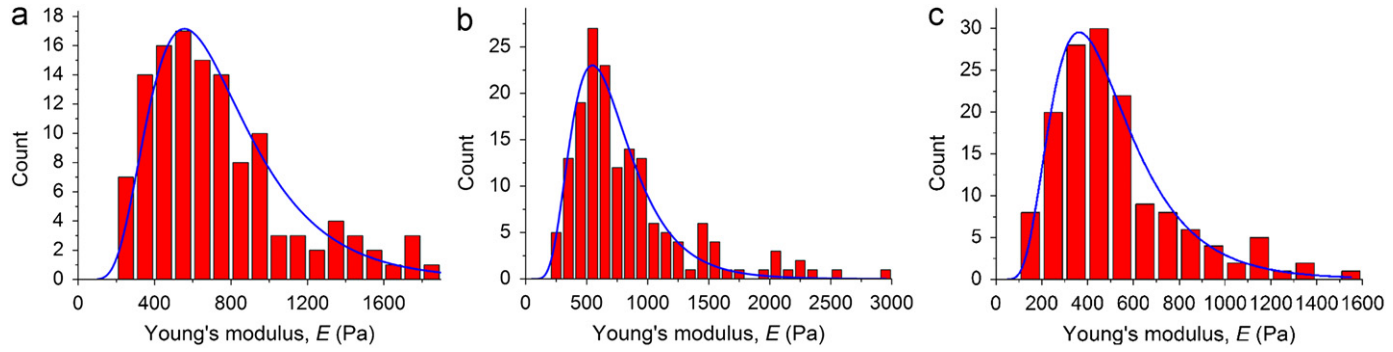

Fig. 3. Histograms of Young's modulus *E* for Vero cells with log-normal fitting. (a) single cells; (b) cells in wound; and (c) cells in monolayer.

sometimes can form a second layer after the prolonged cultivation, which was also observed on confocal images (data not shown).

3.2. Measured Vero cells stiffness depends on the indentation depth

The indentation range for fitting force curves with the Hertz model was selected to minimize contributions of the substrate effect (Li et al., 2008). The typical force curves for different cell states (non-confluent, migrating in wound and cells in monolayer) are presented in Fig. 2a–c; all measurements were conducted at the same 1 μm/s loading rate. The estimated Young's modulus depended on the indentation depth (Fig. 2d–f). At 500–1000 nm indentation the increase of Young's modulus started due to a substrate effect. The 500 nm value is shown to be a sufficient penetration depth for the application of the Hertz model in several studies (Lekka et al., 2011; Li et al., 2008; Takai et al., 2005). On the other hand, if the indentation was less than 100 nm, we observed rather large and scattered values of E (Fig. 2d–f). Such indentation dependence has been presented in many studies on mechanical properties of living cells by AFM (Mahaffy et al., 2000; Rico et al., 2005; Takai et al., 2005), so it could be an intrinsic cell property, rather than an experimental error. E values obtained by force curve fitting as a function of indentation depth (limit of fitting) have a similar indentation dependence, but the graph is smoother (Fig. 2g–i). So, we used E values, obtained from fitting the first 500 nm of indentation at the force curve to reduce the errors, generated by random deflection fluctuations.

3.3. Distributions of Young's modulus values are log-normal

Young's modulus data in experiments, done using all cell states (approximately 50 cells in each state were analyzed), were well fitted by a log-normal distribution (Fig. 3). We checked the normality of the log-transformed data using the Shapiro–Wilk test. The p-values 0.24, 0.056, and 0.28 were obtained for confluent, single and migrating cells respectively. This indicates that the examined data are distributed normally (0.05 significance level) and the raw data are distributed log-normally. Thus we analyzed not only the arithmetic means but also the geometric means of the discussed distributions. The mean of the log-transformed is equal to the geometric mean of the primary data. The exponentiated standard deviation of the log-transformed data gave us multiplicative log-normal standard deviation.

3.4. Confluency affects Vero cell Young's modulus

The geometric mean of elastic modulus of Vero cells in the monolayer was 1.4–1.7 times lower than that of single non-confluent cells and cells migrated in the experimental wound (Table 1). Based on the Mann–Whitney test, the population of cells in monolayer was significantly distinguishable from the two others ($p < 0.0001$), while the latter ones were not significantly distinguishable from each other ($p = 0.14$). The multiplicative standard deviations for all cell types were similar ($\sim 1.6\times$).

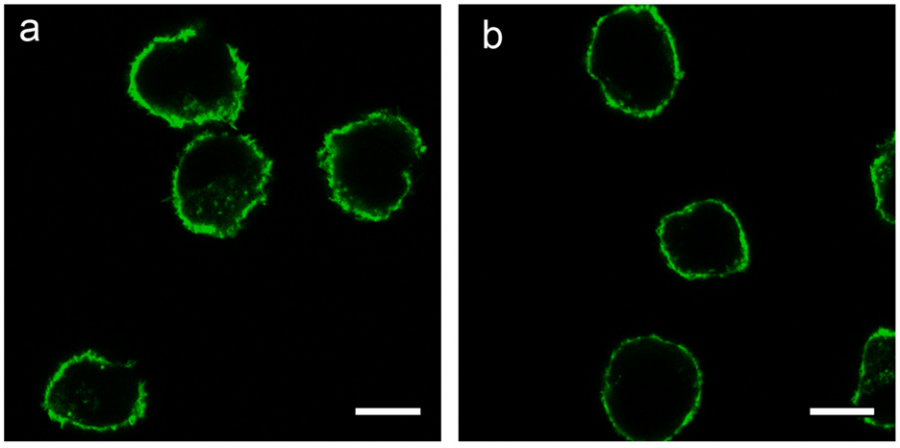

Fig. 4. Actin cytoskeleton in suspended Vero cells, confocal microscopy sections near the middle planes of cells. (a) Non-confluent cells and (b) cells in monolayer. The scale bars represent 10 μm. Mainly cortical actin (layer underneath the plasma membrane) is stained.

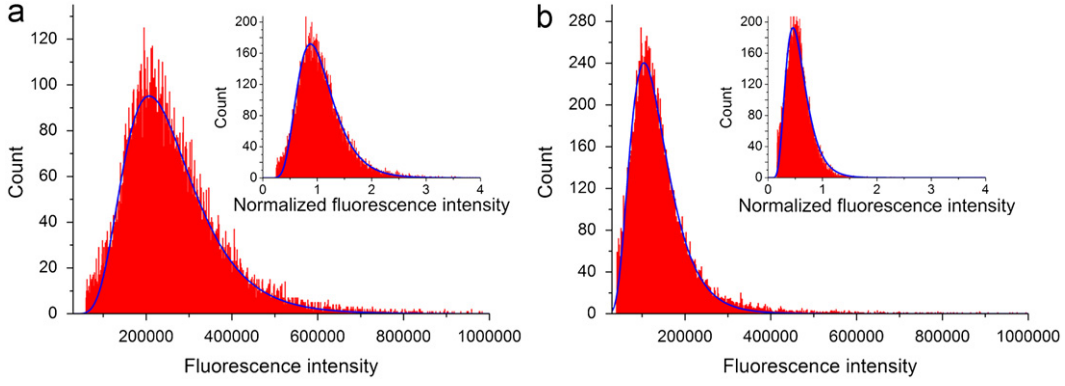

Fig. 5. Flow cytometric measurements of cortical actin amount and the histogram plots. (a) Non-confluent cells, and (b) cells in monolayer. Alexa Fluor 488 phalloidin staining, green fluorescence channel, integral signal. Solid lines represent log-normal fitting curves. The inset shows the distributions of normalized cortical actin amount.

Although arithmetic mean is not an adequate parameter to describe log-normally distributed data, it is commonly used in data processing and thus worth discussing. The difference between the arithmetic means of elastic modulus of single, migrating in experimental wound and confluent cells was the same (1.4–1.6 times) (Table 1). For measurements conducted on the same cell (3–5 random force curves in the area near the center of the cell) standard deviation is rather small, typically less than 100 Pa, which is not more than 20% of the arithmetic mean.

3.5. Actin distribution in Vero cells in different states measured by flow cytometry

To further investigate the impact of the F-actin amount on the obtained Young's modulus values we conduct the flow cytometric measurements on the resuspended confluent and non-confluent Vero cells. The confocal microscopy images showed (Fig. 4), that suspended Vero cells retain the cortical actin network, while they lack stress fibers. Similar results have been obtained previously for other cells in suspension (Guck et al., 2005). Thus the amount of F-actin measured by the flow cytometry in terms of fluorescence intensity mainly reflects the amount of the cortical actin in the cells. Fig. 5 shows the distribution of fluorescence intensity for non-confluent cells and cells in monolayer. In consistent with the force spectroscopy data, the distributions were log-normal ($p=0.39$ and 0.25), while the geometric mean was significantly lower (1.8 times, $p<0.001$, the Mann–Whitney test) for cells in monolayer, than that for non-confluent cells. We also found, that integral forward scatter intensities, that are proportional to the cell size, were also log-normally distributed. The distributions, for both investigated cell states, were very similar ($p=0.79$, the Mann–Whitney test). This means that the overall cell size (volume) was not modulated by the cell state. The log-normal distribution shape was also retained ($p=0.12$ and 0.17) for fluorescence intensities values divided by forward scatter intensities (see insets in Fig. 5).

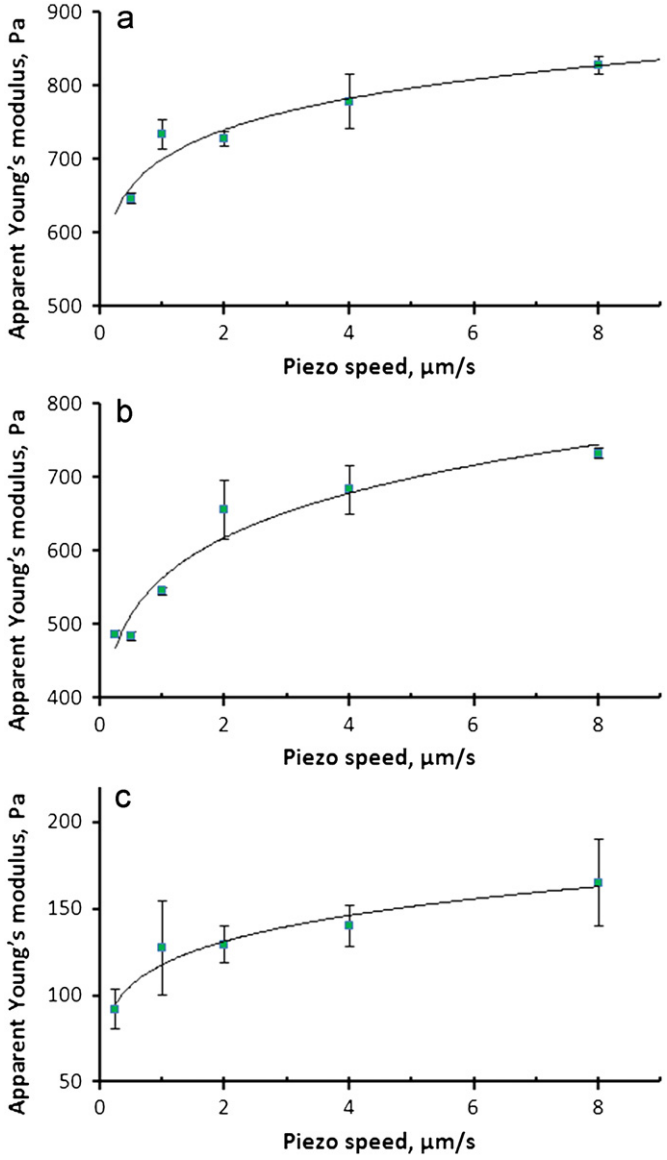

Fig. 6. Typical dependences of the elastic modulus on the force curve speed (piezo speed) for Vero cells, the error bars indicate standard deviations. (a) Single non-confluent cells, (b) cells migrating in wound, and (c) cells in monolayer.

3.6. Vero cell viscoelastic properties are modulated by confluency

Viscoelastic behavior of cells was characterized by measuring their Young's modulus at varying indentation rates (0.25–8 μm/s). We found, that for all three cell states E values increased significantly at higher indentation rates. The observed increase in the apparent modulus followed a weak power law (the equation $k(v)=Av^{\alpha}$, v—the piezo speed), with exponents $\alpha=0.08\pm0.02$, 0.1 ± 0.03, and 0.15 ± 0.03 for single non-confluent, migrating in the experimental wound cells and cells in monolayer respectively. The difference between the α values for cells in monolayer and other cell states is statistically significant ($p<0.05$). Typical indentation rate dependences are shown in Fig. 6. We also measured loss tangents (η) by applying low-amplitude sinusoidal perturbations with 0.3 Hz frequency to the scanner Z-electrodes, when the cantilever was at ~500 nm indentation. We obtained very similar η values for all cell states: 0.17 ± 0.06, 0.20 ± 0.07, and 0.18 ± 0.06 (single non-confluent, migrated in the experimental wound cells and cells in monolayer respectively). Thus, all cells in their studied states demonstrated a mostly solid behavior.

4. Discussion

Young's modulus measurement by AFM has been suggested as a powerful method to study processes that involve cytoskeleton reorganization, for example, for distinguishing the cancerous cells (Cross et al., 2007; Lekka et al., 2011, 2012). However, numerous factors, like substrate stiffness, surface modifications and cell ageing, may interfere with the measured stiffness values of the cultivated cells, and therefore result in incorrect prognoses. Many factors that potentially influence the cell Young's modulus are still unknown.

In this study we investigated the effects of confluency on cell mechanical properties. We compared the elastic properties of Vero cells, growing in monolayer to that of single non-confluent cells and cells migrating in the experimental wound (Table 1). We found that the stiffness of cells growing in monolayer is

Table 1
Young's moduli calculated for Vero cells in different states.

Parameter	Single non-confluent	Migrating in wound	In monolayer
Geometric mean (Pa)	650	730	460
Multiplicative standard deviation	1.63	1.67	1.63
Arithmetic mean (Pa)	730	840	510
Standard deviation (Pa)	370	490	270

significantly lower. On the other hand the stiffness of single non-confluent cells and cells migrating in wound were similar. This similarity suggests that cells can easily change their cytoskeleton structure after leaving monolayer to a movable state. Thus we have shown that the confluency (monolayer density) of the seeded cells is an important factor that influences cell stiffness in addition to other factors, like substrate stiffness and modifications, cell ageing and disease state (Franze et al., 2009; Lekka et al., 2012; Takai et al., 2005).

The difference in Young's modulus of cells in a motile state (single non-confluent and migrating in wound) and cells in monolayer measured by AFM may be a consequence of differences in cortical actin network structure. Indeed, our flow cytometry experiments reflected the differences in the amount of cortical actin in confluent and non-confluent Vero cells (Fig. 5), in good agreement with our force spectroscopy data (Fig. 3). In several recent works it has been shown that at small indentations (500 nm and less) actin cortex is the major contributor to the measured cell elasticity (Nawaz et al., 2012; Pogoda et al., 2012; Solon et al., 2007). Our results agree with those obtained in a prior study (Kole et al., 2005). Mechanical stiffening of migrating Swiss 3T3 fibroblasts was shown in this work with the use of intracellular microrheology and scratch-wound assay.

The migrating cells are polarized and complex regulatory pathways spatially and temporally determine the migration process (Ridley et al., 2003). Cytoskeleton reorganization is an essential part of motility. Presumably, actin polymerization and the formation of an entangled cortical network, detected as stiffening of migrating cells by AFM, facilitate migration by providing mechanical stability to cellular protrusions (Kole et al., 2005). Cells in monolayer remain immobile and constantly receive signals (mechanical and molecular) from neighbor cells, which lead to changes in cytoskeleton structure (Holle and Engler, 2011; Yeung et al., 2005). Also, these cells have comparable contact area with both hard substrate and soft neighboring cells. So, the relative influence of substrate, leading to stiffening of the cells (Solon et al., 2007), may be reduced.

Young's modulus values for all the studied cell states (single, migrating in wound and confluent) were well fitted by the log-normal distribution (Limpert et al., 2001). Similar results were previously obtained in several works with not only AFM measurements of mechanical properties (Cross et al., 2007; Hiratsuka et al., 2009; Ketene et al., 2011; Mizutani et al., 2008), but also magnetic tweezers assay (Alenghat et al., 2000; Swaminathan et al., 2011), magnetic twisting cytometry (Fabry et al., 2001), laser tracking microrheology and two-point microrheology (Hoffman et al., 2006). We suppose that the observed log-normal distribution of Young's modulus values may result from the log-normal distribution of cortical actin network density or its level of crosslinking. Our flow cytometry data confirm the former suggestion (Fig. 5). Indeed, the concentrations of many cell mRNAs, proteins, and metabolites are distributed close to log-normal (Furusawa et al., 2005; Lu and King, 2009). It was shown by laser scanning cytometry that the distribution of F-actin concentration in fibroblasts is also fitted by log-normal distribution (Guck et al., 2005). Log-normal distribution has some features distinct from normal distribution. For characterization and comparison of log-normally distributed data it is appropriate to use mean geometric and multiplicative standard deviation, rather than arithmetic mean and regular standard deviation (Limpert et al., 2001).

For elastic materials the measured response does not depend on the deformation rate. We found that the measured cell stiffness depends on the loading rate, according to a weak power law. The exponent α value for cells in monolayer (0.15) was greater than α value for non-confluent (0.08) and migrating in wound cells (0.1). All the values were in good agreement with the published data for small deformations (Nawaz et al., 2012). This difference apparently indicates that for a monolayer the observed decrease in elastic modulus is accompanied by an increase in contribution of viscous response. However we obtained very similar loss tangent values (at 0.3 Hz) for all cell states, showing mostly solid behavior ($\eta < 1$), like many other mammalian cells (Alcaraz et al., 2003).

The interconnection between cell confluency and stiffness is of special interest particularly for Vero cells. Vero cells passaged at sub-confluence level have a less aggressive tumorigenic phenotype with the increase in passage levels, than randomly passaged cells (without confluence control) (Manohar et al., 2008). The latter ones are able to form a monolayer during their growth which, as we have shown here, decreases their Young's modulus. It is also known, that in many cases cancer cells are characterized by significantly lower stiffness than normal cells, reflecting changes in the actin cytoskeleton structure (Cross et al., 2007; Lekka et al., 2012). So, presumably remaining in monolayer with a relatively low Young's modulus could be connected with the enhancement of tumorigenicity of randomly passaged Vero cells.

In summary, we demonstrated that the viscoelastic properties of cells are modulated by their motility and intercellular interactions in confluent monolayer. In line with previous studies we demonstrated that Young's modulus values of cells are well fitted by the log-normal distribution, which may be a fundamental property of living cell biomechanics. Additionally, we demonstrated that the amount of cortical actin in cultivated cells is also distributed log-normally (Fig. 4). Thus, for characterization and comparison of log-normally distributed data it is appropriate to use mean geometric and multiplicative standard deviation, rather than arithmetic mean and regular standard deviation (Limpert et al., 2001). In future it would be interesting to examine the impact of confluence on mechanical properties for cells growing on soft substrates and substrates coated with extracellular matrix proteins.

Conflict of interest statement

The authors have no conflicts of interest to declare.

Acknowledgments

The authors thank Ms. Olga Vorontsova for help with obtaining confocal microscopy data and Ms. Lisa Trifonova for proofreading the manuscript. This work was supported by the Russian Ministry of Education and Science (Contract 16.740.11.0373, K.S.) and a Knowledge Avant-garde Award from AstraZeneka (O.S.) and partially supported by RFBR Grant 13-04-01570 (K.S.).

Appendix A. Supporting information

Supplementary data associated with this article can be found in the online version at http://dx.doi.org/10.1016/j.jbiomech.2013.01.022.

References

Alcaraz, J., Buscemi, L., Grabulosa, M., Trepat, X., Fabry, B., Farré, R., Navajas, D., 2003. Microrheology of human lung epithelial cells measured by atomic force microscopy. Biophysical Journal 84, 2071–2079.

Alcaraz, J., Buscemi, L., Puig-de-Morales, M., 2002. Correction of microrheological measurements of soft samples with atomic force microscopy for the hydrodynamic drag on the cantilever. Langmuir 18, 716–721.

Alenghat, F.J., Fabry, B., Tsai, K.Y., Goldmann, W.H., Ingber, D.E., 2000. Analysis of cell mechanics in single vinculin-deficient cells using a magnetic tweezer. Biochemical and Biophysical Research Communications 277, 93–99.
Barrett, P.N., Mundt, W., Kistner, O., Howard, M.K., 2009. Vero cell platform in vaccine production: moving towards cell culture-based viral vaccines. Expert Review of Vaccines 8, 607–618.
Costa, K.D., 2006. Imaging and probing cell mechanical properties with the atomic force microscope. Methods in Molecular Biology 319, 331–361.
Cross, S.E., Jin, Y.S., Rao, J., Gimzewski, J.K., 2007. Nanomechanical analysis of cells from cancer patients. Nature Nanotechnology 2, 780–783.
Efremov, Y.M., Bagrov, D.V., Dubrovin, E.V., Shaitan, K.V., Yaminskii, I.V., 2011. Atomic force microscopy of animal cells: advances and prospects. Biophysics 56, 257–267.
Ehrlich, H.J., Berezuk, G., Fritsch, S., Aichinger, G., Singer, J., Portsmouth, D., Hart, M.K., et al., 2012. Clinical development of a Vero cell culture-derived seasonal influenza vaccine. Vaccine 30, 4377–4386.
Engel, A., Muller, D.J., 2000. Observing single biomolecules at work with the atomic force microscope. Nature Structural Biology 7, 715–718.
Fabry, B., Maksym, G.N., Shore, S.A., Moore, P.E., Panettieri, R.A., Butler, J.P., Fredberg, J.J., 2001. Selected contribution: time course and heterogeneity of contractile responses in cultured human airway smooth muscle cells. Journal of Applied Physiology 91, 986–994.
Franze, K., Reichenbach, A., Käs, J., 2009. Biomechanics of the CNS. In: Kamkim, A., Kiseleva, I. (Eds.), Mechanosensitivity of the Nervous System. Springer, Netherlands, pp. 173–213.
Furusawa, C., Suzuki, T., Kashiwagi, A., Yomo, T., Kaneko, K., 2005. Ubiquity of log-normal distributions in intra-cellular reaction dynamics. Biophysics 1, 25–31.
Graham, H.K., Hodson, N.W., Hoyland, J.A., Millward-Sadler, S.J., Garrod, D., Scothern, A., Griffiths, C.E.M., et al., 2010. Tissue section AFM: in situ ultrastructural imaging of native biomolecules. Matrix Biology 29, 254–260.
Guck, J., Schinkinger, S., Lincoln, B., Wottawah, F., Ebert, S., Romeyke, M., Lenz, D., et al., 2005. Optical deformability as an inherent cell marker for testing malignant transformation and metastatic competence. Biophysical Journal 88, 3689–3698.
Hiratsuka, S., Mizutani, Y., Tsuchiya, M., Kawahara, K., Tokumoto, H., Okajima, T., 2009. The number distribution of complex shear modulus of single cells measured by atomic force microscopy. Ultramicroscopy 109, 937–941.
Hoffman, B.D., Massiera, G., Van Citters, K.M., Crocker, J.C., 2006. The consensus mechanics of cultured mammalian cells. Proceedings of the National Academy of Sciences 103, 10259–10264.
Holle, A.W., Engler, A.J., 2011. More than a feeling: discovering, understanding, and influencing mechanosensing pathways. Current Opinion in Biotechnology 22, 648–654.
Ketene, A.N., Schmelz, E.M., Roberts, P.C., Agah, M., 2011. The effects of cancer progression on the viscoelasticity of ovarian cell cytoskeleton structures. Nanomedicine: Nanotechnology, Biology and Medicine 8, 93–102.
Kole, T., Tseng, Y., Jiang, I., Katz, J., Writz, D., 2005. Intracellular mechanics of migrating fibroblasts. Molecular Biology of the Cell 16, 328–338.
Kuznetsova, T.G., Starodubtseva, M.N., Yegorenkov, N.I., Chizhik, S.A., Zhdanov, R.I., 2007. Atomic force microscopy probing of cell elasticity. Micron 38, 824–833.
Lai, Y.M., Stein, D.E., Soong, Y.K., Tang, Y.X., Grifo, J., Malter, H.E., Talansky, B.E., et al., 1992. Evaluation of Vero cell co-culture system for mouse embryos in various media. Human Reproduction 7, 276–280.
Lekka, M., Gil, D., Pogoda, K., Dulińska-Litewka, J., Jach, R., Gostek, J., Klymenko, O., et al., 2011. Cancer cell detection in tissue sections using AFM. Archives of Biochemistry and Biophysics 518, 151–156.
Lekka, M., Pogoda, K., Gostek, J., Klymenko, O., Prauzner-Bechcicki, S., Wiltowska-Zuber, J., Jaczewska, J., et al., 2012. Cancer cell recognition—mechanical phenotype. Micron 43, 1259–1266.
Li, Q.S., Lee, G.Y.H., Ong, C.N., Lim, C.T., 2008. AFM indentation study of breast cancer cells. Biochemical and Biophysical Research Communications 374, 609–613.
Limpert, E., Stahel, W.A., Abbt, M., 2001. Log-normal distributions across the sciences: keys and clues. BioScience 51, 341–352.
Lodish, H., Berk, A., Zipursky, S.L., Matsudaira, P., Baltimore, D., Darnell, J., 2000. Molecular cell biology. In: Freeman, W.H. (Ed.), Cell. W.H. Freeman and Company, New York, pp. 973.
Lu, C., King, R.D., 2009. An investigation into the population abundance distribution of mRNAs, proteins, and metabolites in biological systems. Bioinformatics 25, 2020–2027.
Macfarlane, D.E., Sommerville, R.G., 1969. VERO cells (*Cercopithecus aethiops* kidney)—growth characteristics and viral susceptibility for use in diagnostic virology. Archiv für die gesamte Virusforschung 27, 379–385.
Mackay, J.L., Keung, A.J., Kumar, S., 2012. A genetic strategy for the dynamic and graded control of cell mechanics, motility, and matrix remodeling. Biophysical Journal 102, 434–442.
Mahaffy, R.E., Shih, C.K., MacKintosh, F.C., Käs, J., 2000. Scanning probe-based frequency-dependent microrheology of polymer gels and biological cells. Physical Review Letters 85, 880–883.
Maniar, A.C., Williams, T., Anand, C.M., Hammond, G.W., 1990. Detection of verotoxin in stool specimens. Journal of Clinical Microbiology 28, 134–135.
Manohar, M., Orrison, B., Peden, K., Lewis, A.M., 2008. Assessing the tumorigenic phenotype of VERO cells in adult and newborn nude mice. Biologicals 36, 65–72.
Menezo, Y.J.R., Guerin, J., Czyba, J., 1990. Improvement of human early embryo development in vitro by coculture on monolayers of Vero cells. Biology of Reproduction 42, 301–306.
Mizutani, Y., Tsuchiya, M., Hiratsuka, S., Kawahara, K., Tokumoto, H., Okajima, T., 2008. Elasticity of living cells on a microarray during the early stages of adhesion measured by atomic force microscopy. Japanese Journal of Applied Physics 47, 6177–6180.
Nawaz, S., Sánchez, P., Bodensiek, K., Li, S., Simons, M., Schaap, I.A.T., 2012. Cell visco-elasticity measured with AFM and optical trapping at sub-micrometer deformations. PLoS One 7, e45297.
Pogoda, K., Jaczewska, J., Wiltowska-Zuber, J., Klymenko, O., Zuber, K., Fornal, M., Lekka, M., 2012. Depth-sensing analysis of cytoskeleton organization based on AFM data. European Biophysics Journal 41, 79–87.
Rico, F., Roca-Cusachs, P., Gavara, N., Farré, R., Rotger, M., Navajas, D., 2005. Probing mechanical properties of living cells by atomic force microscopy with blunted pyramidal cantilever tips. Physical Review E 72, 21914.
Rico, F., Wojocikiewicz, E.P., Moy, V.T., 2008. Atomic force microscopy studies of the mechanical properties of living cells. In: Tomitori, M., Bhushan, B., Fuchs, H. (Eds.), Applied Scanning Probe Methods IX. Springer, Berlin Heidelberg, pp. 89–109.
Ridley, A.J., Schwartz, M.A., Burridge, K., Firtel, R.A., Ginsberg, M.H., Borisy, G., Parsons, J.T., et al., 2003. Cell migration: integrating signals from front to back. Science 302, 1704–1709.
Rotsch, C., Radmacher, M., 2000. Drug-induced changes of cytoskeletal structure and mechanics in fibroblasts: an atomic force microscopy study. Biophysical Journal 78, 520–535.
Solon, J., Levental, I., Sengupta, K., Georges, P.C., Janmey, P.A., 2007. Fibroblast adaptation and stiffness matching to soft elastic substrates. Biophysical Journal 93, 4453–4461.
Starodubtseva, M.N., 2011. Mechanical properties of cells and ageing. Ageing Research Reviews 10, 16–25.
Strober, W., 2001. Trypan blue exclusion test of cell viability. In: Coligan, J.E., Kruisbeck, A.M., Margulies, D.H., Shevach, E.M., Strober, W. (Eds.), Current Protocols in Immunology. John Wiley & Sons, Inc., p. Appendix 3B.
Swaminathan, V., Mythreye, K., O'Brien, E.T., Berchuck, A., Blobe, G.C., Superfine, R., 2011. Mechanical stiffness grades metastatic potential in patient tumor cells and in cancer cell lines. Cancer Research 71, 5075–5080.
Takai, E., Costa, K.D., Shaheen, A., Hung, C.T., Guo, X.E., 2005. Osteoblast elastic modulus measured by atomic force microscopy is substrate dependent. Annals of Biomedical Engineering 33, 963–971.
Tanaka, A., Nagayoshi, M., Awata, S., Tanaka, I., Kusunoki, H., 2009. Differentiation of human round spermatids into motile spermatozoa through in vitro coculture with Vero cells. Reproductive Medicine and Biology 8, 169–175.
Valster, A., Tran, N.L., Nakada, M., Berens, M.E., Chan, A.Y., Symons, M., 2005. Cell migration and invasion assays. Methods 37, 208–215.
Ward, K.A., Li, W.I., Zimmer, S., Davis, T., 1991. Viscoelastic properties of transformed cells: role in tumor cell progression and metastasis formation. Biorheology 28, 301–313.
Yeung, T., Georges, P.C., Flanagan, L.A., Marg, B., Ortiz, M., Funaki, M., Zahir, N., et al., 2005. Effects of substrate stiffness on cell morphology, cytoskeletal structure, and adhesion. Cell Motility and the Cytoskeleton 60, 24–34.